Indian Journal of Science and Technology, *Vol 9(42), DOI: 10.17485/ijst/2016/v9i42/99682, November 2016*
ISSN (Print) : 0974-6846
ISSN (Online) : 0974-5645

A Novel Multiple Unsupervised Algorithm for Land Use/Land Cover Classification

T. Vignesh[1], K. K. Thyagharajan[2], D. Murugan[3], M. Sakthivel[4] and S. Pushparaj[4]

[1]Department of Computer Science and Engineering, S. A. Engineering College, Chennai - 600077, Tamil Nadu, India; vigneshthangathurai@gmail.com
[2]R. M. D Engineering College, Kavaraipettai - 601206, Tamil Nadu, India; kkthyagharajan@yahoo.com,
[3]Department of Computer Science and Engineering, M. S. University, Tirunelveli - 627012, Tamil Nadu, India; dhanushkodim@yahoo.com
[4]Department of Geography, University of Madras, Chennai - 600005, Tamil Nadu, India; mathisakthi22@gmail.com, pushparaj.sahadevan@gmail.com

Abstract

Objectives: To classify the satellite images into different land use/land cover classes such as water, building, cropland, forest, etc, to monitor the environmental impacts. **Method:** In this paper, images are grouped into various clusters using a novel SVD trace function clustering algorithm. The clustered samples are used as a training set in a novel unsupervised Ensemble Minimization Learning algorithm (EML) for classification. The main aim of using EML is to classify the forest, vegetative land patterns, build up area in rural and urban areas with the use of best accuracy rate. **Finding:** Our proposed methods provides 90.56% classification rate with low error rate. This EML applies multinomial probit model and ensembles simulated data set and improves the learning of nonlinear relationships between the classified attributes. Multinomial probit model is used to bring all the related possible segmented values to fall into one single category, thus increasing the classification accuracy. Our proposed methods experimented with three different real data sets. The experimental results indicate that our proposed unsupervised model outperforms than the previous techniques. **Application:** It could be using for land use/land cover change detection, under water object identification, coastal area monitoring, etc. **Improvement:** In future it could be apply in video data and could be improve the classification accuracy also.

Keywords: Ensemble Minimization Learning algorithm, Land use/Land Cover Classification, Multinominal Probit Model, SVD Trace Function, Unsupervised Algorithm

1. Introduction

Land use/land cover classification is a fundamental component for the terrestrial ecosystem that plays a major role in exchanging energy, hydrological process and bio-chemical process on the surface of the earth. Forest and vegetation cover refers to the green cover as seen from lowest point of the total statistical surface. This is regarded as an important parameter that decides on regional climate modelling, weather prediction and global weather change studies. A classification of automatic remotely sensed images for crop discrimination was established the highest overall classification accuracy of 92.8%[1,2]. Classification of urban areas is important for monitoring, planning etc. and to study the environmental impact. An Inter-Cluster Separation (ICS) algorithm can be used to get better dithered images in terms of Frequency Weighted Mean Squared Error (FWMSE)[3]. In order to do this; it is advised to classify the urban and rural areas accurately and comprehensively using remote sensing satellite data and the changes in the remotely sensed images can be detected by using Expectation-Maximization-based Level Set (EMLS)[4,5]. Remote sensing is a feasible method to generate vegetation and forest cover images because of its ability to generate impartial and broad data of land surface[6–9].

**Author for correspondence*

This large topographic image seems to possess low quality pixels, false and mixed colouring to a larger degree; making it a challenging task for image classification[10]. The major disadvantage of these large topographical images is its noise and delimiters could reduce the accuracy of classifying it with prior methods and it can be improved by object classification methods. Certain parameters are combined in certain researches like combining color and spatial information with FCM with restricted membership rules[11,12]. In further researches, the membership rules were adjusted and used for determining the weighted factors using weighted FCM clustered algorithm. If the clustering is done based on class center of the topographical maps, color features may not provide a major significance[13–15]. Problems like blur effects, partial-color and graduated color can be eradicated like to a certain extent using fuzzy based technique.

These methods perform well with small topographic images and a larger problem will occur in that image. The cause due to this problem is that, it requires large scaling and long computation of the resultant image for clustering and classification[16–18]. Certain number of distance metric unsupervised and supervised learning algorithms is emerging now-a-days[19, 20]. In many classes, label information is unavailable that makes the supervised learning as an inefficient one[21,22]. To solve this, unsupervised learning using set of clusters with maximum inter cluster severability methods are used[23–25]. Large and complex areas in urban cities and its spatial development can be evaluated by using the strength of remote sensing satellites based on change detection studies[26–30] and the lower resolution data in the images can be detected by using land-cover changes[31–33].

In our method, both clustering and classification is done for large topographical images to analyze the vegetative land patterns. Here, three various timelines were selected in order to cluster the images and classifying it based on the training samples. This is done to find the availability of vegetative land patterns on a specified region and identifying the type of vegetative field e.g., wheat, rice, paddy, etc., through classification. Finally, a third level analysis of shrinkage or increase in vegetative land is done to find the availability of vegetative field in the particular area. Initially, clustering is done using a novel SVD trace function that separates the cluster with less imbalanced clustering region in given topographical image. These clustered samples are further used as classes for a novel unsupervised Ensemble Minimization Learning algorithm (EML) learning. This method uses multinomial probit model or Multinomial Probit Fit (MPF) to avoid the regression fit problems during ensemble learning and categorizing correctly the clustered samples to vegetative land. Tested samples prove that the novel technique is efficient and further the classified labels were used for subtracting the size and dense of vegetative land pattern in a particular region. These above two novel unsupervised algorithms were used for clustering and classification process.

The organization of this paper is represented as follows: Section 2 deals with the proposed methodology and to prepare the topographical image for further stages. Section 3 analyses the clustering and classification principle proposed to improve the level of accuracy of finding the vegetative field. Section 5 presents the experimental results in terms of efficiency and accuracy. Section 6 and section 7, we discuss the results with existing methods and concluding it with remarks.

2. Methodologies

2.1 Study Area

The state province of Tamil Nadu, India covers an area of 130,058 km^2 that comprises a wide variety of ecosystems and landscapes. Tamil Nadu a leading producer of agricultural products in India with a cultivated area of 5.60 million hectares in 2009 - 10 and this is been reducing abundantly. Our study area is based on the district of Kanyakumari, Tamil Nadu. Due to urbanization, the land patterns have reduced strictly and this leads to the degradation in the cultivation of the food crops. The crop field data contains a land pattern of 1000 plots that were collected in between three timelines. The data was collected from http//earthexplorer.usgs.gov/, and http//bhuvan.nrsc.gov.in/. Apart from the vegetation and forest cover, other regions including houses, lakes, roads were included in this larger topographical image. A National Forest Inventory (NFI) method is cost-effective and accurate way to forecast large areas of forest land attributes.

2.2 Feature Extraction

For feature extraction, the dimensionality of the space feature is typically greater than the range of the training set. It is called as Under Sample Problem (USP). A traditional classifier such as LDA (Linear Discriminant Analysis), often fails when faced by USP. One solution is to minimize the feature space's dimensionality by using the

Principal Components Analysis (PCA) or the Multilinear Subspace Analysis (MSA). Unfortunately, some discriminant data is surplus by MSA and PCA. An unequal sized clusters, outliers and noise can be treated by using Alternative Hard C-Means AFCM and Alternative Fuzzy C-Means AHCM method[34–36].

Initially, we create a nearest neighbour region for each sample to model the local geometrical structure of the underlying manifold and initiate Local Differential Scatter Discriminant Criterion (LDSDC). Consequently depends upon LDSDC, a constraint optimization problem with a new objective function is developed. Then, an unconstraint optimization problem is relocated by the optimization problem[37]. Conversely, it's very tough to solve an unconstraint optimization problem. By employing the gradient method on two unknown matrices iteratively and correspondingly is started, the above problem can be solved. This changes us to propose an algorithm that guarantees the objective function meets and an optimal projection matrix is found.

On the other hand an iterative algorithm called LSBFE algorithm was proposed to solve the optimization problem based on two sub-models which is shown in Figure 1. After the objective function meets to a single point, we attain a converged subspace matrix W*. Then, we scheme the samples into a low-dimensional subspace by $Y = W^{*T} X$. LSBFE algorithm consists of two layer structures such as output and input layer.

Instead of conventional method of Eigen value decomposition, a new proposed LSBFE is introduced. This algorithm guarantees the union of iterative process. The new algorithm has been tested on forest, vegetation land patterns, lakes, reservoirs etc.

2.3 Classification Model

Larger topographical maps can be segmented to cluster the image than classifying it. Thus, classification is taken to be a preliminary concept in our proposed approach that clusters the given land pattern of two varied timelines into several clusters using SVD trace function. SVD is an approach of an advanced linear algebra[38]. This is followed by classification of the clustered samples based on proposed EML algorithm that uses MPF to classify accurately the vegetative land patterns. This is further applied to third level of the resultant model that uses a similarity measure to find the total vegetative land area shown in Figure 2.

1. For each training sample, a nearest neighbour region was obtained. After that calculate scatter matrices S_b and $\tilde{S}_w$
2. Initialize Λ as Identity matrix Λ_0 and Initialize W as an arbitrary orthogonal matrix W_0

Repeat {

3. Calculate $\nabla_w L(W_{i-1,} \Lambda_{i-1})$.

$$\nabla_w L(W, \Lambda') = AW + A^T W + 2W(\Lambda' \circ (W^T W - I) \circ \Lambda')^T + 2W(\Lambda' \circ (W^T W - I) \circ \Lambda')$$

4. Update W_i

$$W_i = W_{i-1} - \eta \nabla_W L'(W_{i-1}, \Lambda_{i-1}) + \alpha \Delta W_{i-2}$$

5. Compute $\nabla_\Lambda L(W_i, \Lambda_{i-1})$

$$\nabla_\Lambda L(W', \Lambda) = 2\Lambda \circ (W^T W' - 1) \circ (W^T W' - I) - 2\varepsilon\Lambda + (2\Lambda \circ (W^T W' - I) \circ (W^T W' - I) - 2\varepsilon\Lambda)^T - diag(2\Lambda \circ (W^T W' - I) \circ (W^T W' - I) - 2\varepsilon\Lambda)$$

6. Update Λ_i

$$\Lambda_i = \Lambda_{i-1} + \xi \nabla_\Lambda L(W_i, \Lambda_{i-1}) + \beta \Delta \Lambda_{i-2}$$

7. i=i+1}

Until the following criterion is satisfied:

$$\left\| W^T W - 1 \right\|_F^2 \leq \epsilon$$

8. $W^* = W_i$
9. Project the samples into a low-dimensional subspace

$$Y = W^{*T} X$$

Figure 1. LSBFE algorithm.

3. Land Pattern Classification Model

The land pattern classification model consists of three modules that include three stages of processing the larger topographical maps. In the initial stage, the image is clustered, in the intermediate stage it is classified and in final stage a similarity measure is applied to identify the real objective of the research.

3.1 SVD Trace Clustering Algorithm

SVD is an approach of an advanced linear algebra. The classification accuracy is influenced significantly by the training set of data in case of classification problems. But imbalanced class distribution of data is frequently occur in real-time applications i.e., a small amount of data are in minority class and a large amount of the data are in majority class. During this case, the classifier inclines to predict that almost all of the incoming data belongs to the majority class when each and every data are used to be the

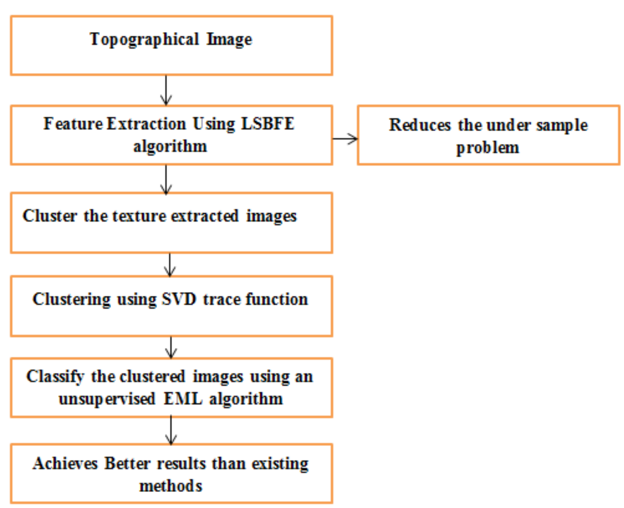

Figure 2. Texture extraction and classification procedure.

training data. Hence, it's vital to choose the appropriate training data for classification within the unbalanced class distribution issue. In a training dataset, there will be more samples in one class when compared to other which happened during the issue of imbalanced class distribution. A little amount of samples is occupied by minority class whereas large amount of samples is occupied by majority class in an imbalanced dataset. During this case, a classifier sometimes inclines to ignore the minority class fully and predict the majority class samples. These problems can be overcome by using an unsupervised SVD Trace clustering algorithm[39]. Unsupervised learning is an art that manifest the geometric relationship between the data. Due to the presence of imbalanced clusters between the clustered images, we go for Neighbourhood Component Analysis (NCA). To achieve better closeness and to reduce the unbalanced clusters, Singular Value Decomposition (SVD) matrix is applied as an objective function over the unsupervised samples. This can achieve the closeness as well as the balanced clusters in the resultant image.

In a classification task, the impact of imbalanced class distribution issue is frequently disregarded. Numerous studies concentrated on enhancing the classification accuracy yet did not consider the imbalanced class distribution issue. Subsequently, the classifiers which are developed by these studies lose the capacity to accurately foresee the correct decision class for the datasets in the minority class samples which the amount of minority class samples is lower than the majority class samples[40]. The issue of imbalanced data is frequently associated with asymmetric costs of misclassifying elements of various classes. Moreover at learning time, the true costs of misclassification may be unidentified and the test data distribution might differ from that of the learning samples. The imbalanced data set has some issues which are caused by the normal classifier for example; 1. The classifier will work on data drained from the same distribution as the training data. 2. Accuracy is increased. In this study, we propose a novel cluster-based SVD Trace algorithm to overcome the problems of imbalanced clusters.

Singular Value Decomposition (SVD) can be appeared at from three equally well-suited standpoint. On the one hand, we can see it as a method for translating a set of uncorrelated variables by a correlated one that better expose the different relationships along with the original data items[41]. Simultaneously, SVD is a method for identifying and ordering the dimensions along which data points reveal the most discrepancy. This binds in to the third method of viewing SVD, which is that once we have recognized where the most difference is, it's feasible to determine the best estimation of the original data points using fewer dimensions. Hence, data reduction is obtained by using SVD method.

The pseudo code of the SVD trace clustering is shown in Figure 3. This unsupervised NCA uses cluster SVD matrix as a trace or objective function that is expressed as:

$$OF\left(V,S\right)=tr\left(S^{T}PS\right) \tag{1}$$

This SVD trace function having cluster SVD matrix is represented S as:

$$S=\{s_{ij}\}_{n\times k},\, where \begin{cases} \dfrac{1 \quad x_i \in C_j}{0 \quad otherwise} \end{cases} \tag{2}$$

Increasing the SVD trace function directly increases the imbalanced cluster having numerous amount of sample. The numerous samples can be reduced by increasing the threshold of the edges using Otsu threshold over the clustered samples. This leads to the reduction of acquiring large number of cluster for the given topographical image. Thus Otsu threshold of SVD trace function leads to less number of clustered samples that is defined as:

$$s=O\left(S^{T}PS\right)=O(S^{T}).P.O(S) \tag{3}$$

The Equation (1) and (2) can be improved to:

$$OF\left(V,s_o\right)=tr\left(s_o^{t}ps_o\right) \tag{4}$$

Where,

$$s_o=\{s_{ij}\}_{n\times k},\, where \begin{cases} \dfrac{1 \quad x_i \in C_j}{0 \quad otherwise} \end{cases} \tag{5}$$

Thus the cluster size is reduced using Otsuthres holding over an objective function defined in Equation

Pseudo code for clustering

1. *Read the given the satellite image*
2. *Create an objective function using SVD matrix*

   $OF\ V,S\ =tr\ S^{T}PS$

   Where,

   P = *probability matrix between different points in disjoint clusters*

   S = clustered SVD matrix
3. *Increase the threshold level of the edges and apply trace function over it*
4. *Penalty factor: Apply sparse matrix over the threshold traced samples and remove the zero-valued samples over the clusters.*
5. *Obtain the weighted clusters with reduced irrelevant clusters*
6. *If non linearity is present in the clustered samples*
7. *Obtain the weighted clusters with reduced irrelevant clusters*
8. *If non linearity is present in the clustered samples*
   a. *Apply neighbourhood Klein Graph over the reduced weight clustered samples*
   b. *Reduce the distance between the clustered samples by bringing out neighbourhood relation*
9. *Group the crowded clusters*
10. *End the process.*

Figure 3. SVD trace clustering of large topographical images.

(1). Reduction in cluster size could reduce the unbalancing of clustered samples in the target space. Further reduction in dimensionality could be achieved by throwing away the irrelevant neighbourhood components using sparse identification matrix. Application of sparse matrix over Equation (5) helps in finding out the zero valued clusters in the clustered image. This reduces further the clustered irrelevant or zero valued samples and is shown in Equation (6):

$$S_o = sparse(s_o) \tag{6}$$

To reduce this and to achieve the balancing in cluster, S_o with zero values in the clusters are eliminated. Non-zero valued clusters helps in reducing the redundant information with better qualified clusters. The clustered size with reduced clusters could thus be defined as in Equation (7):

$$OF\left(V,N\right) = tr\left(N^T PN\right) \tag{7}$$

The weighted clustered matrix N can be written as in Equation (8):

$$Z = [z_1, z_2, ..., z_k] \tag{8}$$

The usage of sparse matrix helps in reducing the overfitting problem in weighted clustered matrix with t^{th} column. Here the overfitting is avoided using a penalty factor called sparse matrix. Thus, the unsupervised NCA problem could be formulated with a transformation, **A**:

$$\max_{N^T PN} tr\left(N^T PN\right) - \xi \left\|\mathrm{A}\right\|^2 \tag{9}$$

Maximizing this trace function could increase the expected number of correctly classified points also but non-linearity arises when maximizing the trace function [qin 2015]. This non-linearity is previously avoided through Equation (4)-(6), through thresholding and sparse matrix technique. As reported in [qin 2015], further iterative approach to calculate the A and N is avoided using this technique. This is time consuming and after carrying out this we found a slight misalignment in clustered samples. So, we considered unit neighbourhood graph technique called Klein Graph technique that provides an interconnection between the neighbourhoods clustered samples. Using same edge set and vertex set, with a pair of vertices lying in a distance K can bring closely or can bring an interconnection between the relevant clustered set. N can be regarded as an adjacency matrix with parameters like (v, K, λ, μ) for a neighborhood Klein Graph, G_K. The adjacency matrix for G_1 of the nearest cluster G_2 for mapping is shown in Equation (10):

$$\frac{1}{\mu}(\mathrm{A}^2 - KI - \lambda\mathrm{A}) \tag{10}$$

The distance between the clusters defined in terms of its distance K is found by the Eigen values which is shown in Equation (11):

$$\frac{1}{2}(\lambda-\mu) \pm \sqrt{(\lambda-\mu)^2 + 4(K-\mu)} \tag{11}$$

The between the clusters in terms of strong regular graphs is defined as:

$$(v - K - 1)\mu = K(K - \lambda - 1) \tag{12}$$

This provides a strong relation between the clustered points in the topographical maps and the clusters are made to get crowded. This increases the accuracy of clustering than previous approaches and the topographical images is processed and designed specifically by this is method.

Clustering is the technique in which the data classes can be separated by similar features and it is also used in data mining. A clustering comes under an unsupervised algorithm and it is different from classification algorithm. So, we proposed a novel EML algorithm to form a clustered pattern. These patterns will classify the vegetative land patterns and buildings, lakes, houses etc. The shape and size of the objects are unknown, so it comes under unsupervised learning. The accuracy of the images can be obtained by the classification.

3.2 EML Classification Algorithm

With the clustered samples, we worked out EML to provide an unsupervised learning on the clustered patterns and correctly classifying the vegetative land patterns. Here the unsupervised operation on clustered samples is performed in three stages. Initial stage includes ensemble learning of the clustered patterns in the finite space. Here the individual decisions of the clusters are not taken into account, whereas group decisions of all the samples are considered. Second stage involves improving the decision making of the ensemble learning using Montgomery-Odlyzko law that uses Eigen value dependency between the clustered samples. In third stage or in third phase, dependency in second stage and classification and weighted averaging for regression in first stage is improved using MPF. The whole process is repeated in loops until all the clustered samples are classified correctly. Using our proposed EML, minimization of error in unsupervised learning is achieved to a larger extent.

Step 1: Initial phase/Ensemble Learning

Ensemble Learning (EL) learns a set of samples rather than individual samples that combines the prediction of all these sampled sets. This ensemble unsupervised classifier error rate better than random guessing of new variables. This learning uses both parametric approximation that optimizes posterior Probability Density Function (PDF) and variation approximation learning where whole function is optimized. The ensemble learning between two probability distribution function (*p,q*) is defined as:

$$EL(q,p) = EL\left\{\ln\frac{q}{p}\right\} = \int_v q(v)\ln\frac{q(v)}{p(v)}dv \tag{12}$$

$EL(q,p)$ Measures the difference between the probability density between the distribution function *p(v) and q(v)*. Here when the cluster values are same, the difference is densities become zero.

The main aim of EL is to reduce the misfit between the PDF of the two clusters and its parametric approximation. The Kullback-Leibler divergence over these two cluster distributions is done to find the posterior PDF approximation that is defined as:

$$EL(q,p) = \int_S\int_\theta q(S,\theta)\ln\frac{q(S,\theta)}{p(\mathrm{X},S,\theta\,|\,\aleph)}d\theta\, dS \tag{13}$$

where, S is the latent variable of the data X from parameter θ for attaining more clarity. q(S, θ) of the posterior PDF is taken simple for achieving better computation. This is achieved by considering selected dependences between the clusters and not all clusters are considered.

Step 2: Decision making/Montgomery-Odlyzko Law

Montgomery-Odlyzko Law considers the statistically identical clusters in the Gaussian unitary ensemble with the cluster dependencies taken using Eigen value spacing. This law considers the empirical observation of the spacing distribution between the successive nontrivial clusters in the vector space. The following equation can be used to satisfy the inequalities between the clusters. For order sequence, the Eigen values are represented as: $\lambda_1 < \ldots < \lambda_n < \lambda_{n+1} < \ldots$ and the normalized spacing between the clusters is given by $S = (\lambda_{n+1} - \lambda_n)/s'$ where $s' = (\lambda_{n+1} - \lambda_n)$ is the mean spacing between the clusters. Thus the probability distribution of the spacing between the clusters is further improved using:

$$p_1(S) = \frac{\Pi}{2} S e^{-\frac{\Pi}{4}S^2} \tag{14}$$

This mean value of weighted distribution further increases the decision making process a more accurate one in ensemble learning. Thus, reducing a rate of error while classifying the clusters and minimizes the error.

Step 3: Regression fit/MPF

At the stage of ensemble unsupervised learning, the error minimized clustered samples further undergoes regression problem. Despite mean value, regression fit is an important problem in unsupervised approach that is been addressed in this research. Here using Multinomial Probit analysis or MPF, we improve the dependency of the same cluster in irrelevant class. To improve the dependency, latent variable is achieved by using the Equation (13) which is as follows:

$$\eta_{pq} = z_p a_q + \xi_{pq} \tag{15}$$

Where z_i, row vector contains independent variables (observed) for the p^{th} decision making cluster variable. This latent variable reduces further the regression fit problems in ensemble unsupervised learning using Equation (15). Thus the rate of error is further reduced to a vast extent thus making this EL as Error Minimization Learning or Ensemble Minimization Learning (EML).

By using this EML algorithm, the error can be minimized and the accuracy of the image is obtained. So, by using the SVD trace and EML algorithm overall accuracy of the image clustered from the topographic image can be improved because the image obtained from the satellite is blurred due to weather disturbances and environmental changes. Then, the error can also be minimized.

4. Results

The following results were achieved for land use/land cover classification (Table 1 and 2, 111).

4.1 Barren Rocky

The rock exposures of changeable lithology frequently lacking and desolate of vegetation and soil cover and not appropriate for agriculture and it is known as barren rocky. It arises at the loose fragments of boulders or amidst hill forests as openings or speckled as inaccessible exposures or as sheet rocks on plains and plateau. It also

Table 1. Various combinations of images of Landsat-8, Liss-3 and AWIFS and its Producer's Accuracy (PA %), User's Accuracy (UA %), Overall Accuracy (OA %)

Class		Landsat-8		Liss-3		AWIFS	
		PA	UA	PA	UA	PA	UA
1	Barren Rocky	99.3	77.8	100.0	97.3	100.0	89.2
2	Built-up Land	99.5	87.3	98.5	89.9	100.0	98.0
3	Cropland	88.6	65.4	72.3	63.8	71.9	49.8
4	Deciduous Forest	88.9	66.4	71.1	69.2	72.4	67.9
5	Fallow Land	78.9	66.0	72.3	65.4	73.2	66.2
6	Forest Blank	99.4	89.2	99.3	90.2	89.2	88.2
7	Forest Plantation	98.5	75.8	92.0	79.8	98.0	79.3
8	Plantation	99.2	89.3	99.4	88.9	97.4	87.9
9	Sandy Area	66.8	45.3	67.3	55.2	67.8	55.1
10	Scrub Land	89.4	77.8	88.3	78.8	88.4	76.6
11	Water	100.0	99.5	100.0	99.5	100.0	98.8
OA/Kappa statistics		92.5/0.887		89.69/0.879		89.59/0.865	

includes brick kilns or gravel pit or quarry. The best results were obtained for Liss-3 (PA = 100.0 % and UA = 97.3%). In general, this land was reliably identified (with PA and UA more than 85%) excluding LANDSAT-8. More importantly, using only Liss-3 and AWIFS images, it was possible to surpass 85% accuracy. This suggests barren rocky is partially occupied in the study area (Table 1).

4.2 Built-up Land

A region of human habitation urbanized because of non-agricultural use and it has a cover of transport, communication utilities and buildings in connection with unoccupied lands and water vegetation is known as built-up land. The best results were obtained for AWFIS (PA = 100 % and UA = 98.0 %). In general, this land was reliably identified (with PA and UA more than 87%) for all combinations. More importantly, using only AWFIS images, it was possible to surpass 98% accuracy. This suggests built-up land is also partially occupied in the study area.

4.3 Cropland

When the satellite imagery is started to be taken, it measures the land which have standing crops at the time of process. There are two types of crops, either Rabi (October-March) or Kharif (June-September) or both the seasons. The best results were obtained for combination Landsat-8 (PA = 88.6% and UA = 65.4%). Generally, this crop was dependably recognized (with PA and UA below 88%) for all combinations. More importantly, using only Landsat-8 images, it was possible to surpass 85% accuracy. This suggests that moreover all croplands were degraded.

4.4 Deciduous Forest

It is a forest at which the tress shack their leaves yearly once and it consists of some deciduous species. The best results were obtained for combination Landsat-8 (PA = 88.9% and UA = 66.4%). In general, this type of forests was reliably identified (with PA and UA below 88%) for all combinations except Landsat-8. More importantly, using only Landsat-8 images, it was possible to surpass 88% accuracy. This suggests that deciduous forest occupied the one-fourth of the study area.

4.5 Fallow Land

This type of land is permitted temporarily to take break without cropping the land for one or more seasons but it should not exceed more than one year. At the time when the satellite imagery is taken for both the seasons, these lands specifically seen that it have lacking of crops. The best results were obtained for combination Landsat-8 (PA = 78.9% and UA = 66.0%). In general, this type of land was reliably identified (with PA and UA below 78%) for all combinations. More importantly, using only Landsat-8 images, it was possible to surpass 78% accuracy. This suggests that moreover a part of fallow lands were occupied the area.

4.6 Forest Blank

It is an openings of amidst forest in which there were no tree is covered in that area. It has the possibilities of various shapes and size as seen on the satellite imagery. The best results were obtained for Landsat-8 (PA = 99.4% and UA = 66.0%). In general, this type of land was reliably identified (with PA and UA has 99% accuracy). More importantly, using only Landsat-8 images (it was possible to surpass 99% accuracy. This suggests that moreover a part of forest blank were occupied the area.

Table 2. Confusion matrix for LANDSAT

	Ground truth													
	Class	**1**	**2**	**3**	**4**	**5**	**6**	**7**	**8**	**9**	**10**	**11**	**UA(%)**	**CE(%)**
	1	415	4	0	0	0	0	0	0	0	0	0	99.2	0.8
	2	0	19123	6	32	19	0	1	48	689	0	0	96.2	3.8
	3	0	13	2999	0	4	0	6	2	115	0	0	95.6	4.4
	4	0	45	0	924	74	4	73	62	117	0	0	72.8	29.4
	5	0	2	0	13	30830	13	345	1200	33	0	4	96.1	3.9
Landsat-8 Image	6	0	1	0	4	156	3647	510	1148	69	0	0	77.0	33.0
	7	0	2	0	2	125	8	4929	234	0	0	0	94.2	5.8
	8	0	4	0	4	356	27	1156	13019	12	4	6	89.5	10.5
	9	0	93	249	916	19	0	67	87	5500	0	17	79.6	20.4
	10	0	25	0	3	20	6	54	43	249	1129	4	74.7	25.3
	11	0	140	0	3	25	2	24	17	317	18	995	65.6	34.4
	PA(%)	100.0	98.5	92.5	49.1	97.6	98.8	69.9	82.3	77.7	98.5	88.6		
	OE(%)	0.0	1.5	7.5	50.9	2.4	1.2	30.1	18.7	22.3	1.5	11.4		

Table 3. Confusion matrix for Liss-3

	Ground truth													
	Class	**1**	**2**	**3**	**4**	**5**	**6**	**7**	**8**	**9**	**10**	**11**	**UA(%)**	**CE(%)**
	1	415	0	0	0	0	0	0	4	0	0	0	99.4	0.8
	2	0	17886	28	132	5	0	0	44	940	0	1	94.2	6.5
	3	0	16	2884	9	8	0	4	3	519	0	1	83.6	16.4
	4	0	509	0	1212	236	2	288	90	1009	1	1	37.3	63.9
	5	0	13	0	6	29866	113	368	1009	25	7	8	95.6	5.9
LISS-3 Image	6	0	4	0	0	128	3276	376	2539	34	0	0	51.9	48.7
	7	0	3	0	2	334	118	4749	408	0	6	0	85.5	15.8
	8	0	39	0	16	758	168	1189	11309	28	9	9	83.9	16.5
	9	0	899	236	493	25	3	15	148	4129	4	49	69.6	31.5
	10	0	23	0	0	179	25	149	208	38	1120	8	64.9	25.3
	11	0	67	4	27	89	14	30	98	399	6	978	57.9	43.6
	PA(%)	100.0	92.3	92.5	64.6	94.8	88.9	66.8	71.8	58.4	97.9	87.6		
	OE(%)	0.0	7.7	7.5	35.4	5.2	11.1	33.2	28.2	41.6	2.1	12.4		

4.7 Forest Plantation

A region in which contains more tress of species which is important for forestry and evoked on a particular land in the forest. It contains casuarinas, bamboo, eucalyptus etc. The best results were obtained for combination AWIFS (PA = 98.9% and UA = 89.3%). In general, this type of land was reliably identified (with PA and UA more than 89%). More importantly, using AWIFS and Landsat-8, it was possible to surpass 89% accuracy. This suggests that moreover a part of forest plantation were occupied the half of the area.

4.8 Plantation

A region in which adopts particular management techniques for agriculture and plant crops according to that. It contains orchards, coconut, coffee, tea, rubber and various nurseries for horticulture. The best results were obtained for combination Liss-3 (PA = 99.4% and UA = 88.9%). In general, this type of land was reliably identified (with PA and UA more than 87%) for all the combinations. More importantly, using all combinations, it was possible to surpass 87% accuracy. This suggests that moreover half part of plantation were occupied the half of the area.

4.9 Sandy Area

Areas which have steadied collections of sand in-site or carried in inland areas or coastal riverine are known as sandy area. These regions are in the form of Channel Islands, sand dunes, beaches, etc. The best results were obtained for combination Landsat-8 (PA = 66.8% and UA = 45.3 %). In general, this type of land was reliably identified (with PA and UA more than 55%) except Landsat-8. It was possible to surpass 70% accuracy. This suggests that moreover a part of sandy area were occupied the one-third of the area.

4.10 Scrub Land

A Land which occupies higher topography such as high grounds or uplands with scrub is known as scrub land. It is normally prostrate to erosion or degradation excluding mountainous terrain or hilly area. The better results were found for Landsat-8 (PA = 89.4% and UA = 77.8 %). In general, this type of land was reliably identified (with PA and UA more than 75%) for all the combinations. It was possible to surpass 85% accuracy. This suggests that moreover a part of scrub land were occupied the half of the area.

4.11 Water

It shows 100% accuracy in the satellite imagery area.

The comparison of various clustering algorithm with our proposed algorithm is shown in Table 5.

The comparison of various unsupervised classification algorithm is shown in Table 4.

5. Discussion

In this paper, classification of land-use and land cover was studied in order to study the changes in the environment in the district of Kanyakumari, Tamil Nadu, India. Various land use/land cover patterns were covered under this study. They are Barren rocky, Built-up, Cropland, Deciduous Forest, Fallow Land, Forest Blank, Forest Plantation, Plantation, Sandy area, Scrub Land and Water. The satellite images such as LANDSAT, Liss-3 and AWFIS were used in our study. LSBFE algorithm is used to defeat under sample problem by extracting the features in the topographical image. These extracted images can be clustered into a group using a novel unsupervised SVD trace clustering algorithm. These clustered images classified using an unsupervised EML algorithm. Here, the learning process of EML can be improved because we cannot find the clustered and classified images perfectly. So, we have to go for decision making process. It can be improved by Montgomery law in which the regression problem can be solved by using multinomial probit analysis. The obtained results were shown in Table 1, 2 and 3 and 4. The Table 1 shows the results obtained from the Landsat-8, Liss-3 and AWFIS satellites images. The overall accuracy of Landsat-8 images was 92.5% and Liss-3 images gives 89.7 % and AWFIS images gives 89.5 %. The obtained results show better accuracy than the existing methods. Figure 4 shows the land use land cover classification result of proposed method. Table 5 and 6 shows proposed methods compared with existing methods. The Producer's accuracy shows the percentage of pixels classified as a specific land cover that really are that land cover. The User's accuracy shows the percentage of reference pixels for a specified land cover that are classified accurately. It is most applicable measure of the actual efficacy of classification in the study area. The formula for kappa co-efficient, User's accuracy and Producer's accuracy is shown in various studies. In image classification method, the accuracy can be assessed by using confusion matrix. In this, the values of classification can be compared with the additional ground truth information. The main strength of this matrix is to determine the errors in the classification.

The particular findings of this study are as follows:

- The vegetative and forest land pattern images were captured by the satellite. At the same time, the buildings, lakes, rivers, reservoirs, houses were also taken into account.
- The images captured from the satellite were clustered into a group. This clustered image contains imbalanced clusters. It can be overcome by using SVD trace function in order to achieve better closeness.
- The clustered images can be classified based on EML learning process. Here, the vegetative land patterns were classified accurately until it satisfies the condition. It achieves great minimization of error.

Table 4. Confusion matrix for AWIFS

	Ground truth													
	Class	**1**	**2**	**3**	**4**	**5**	**6**	**7**	**8**	**9**	**10**	**11**	**UA(%)**	**CE(%)**
	1	415	0	0	0	0	0	0	4	0	0	0	98.4	0.7
	2	0	16889	30	129	6	0	0	44	938	0	1	93.4	5.5
	3	0	14	2877	7	9	0	5	4	521	0	1	81.3	16.2
	4	0	502	0	1200	229	2	281	87	1002	2	1	38.6	64.8
	5	0	16	0	5	29854	108	361	1006	27	9	9	96.4	4.8
AWiFS Image	6	0	3	0	0	123	3256	369	2535	33	0	0	50.5	47.7
	7	0	1	0	3	329	111	4732	400	0	8	0	84.4	14.9
	8	0	34	0	12	750	159	1088	11311	23	9	8	87.6	15.9
	9	0	888	230	489	28	5	14	150	4122	5	46	67.5	32.1
	10	0	22	0	0	172	21	139	200	33	1118	7	65.8	25.6
	11	0	69	5	29	81	16	28	91	395	8	974	56.8	43.4
	PA(%)	100.0	93.7	94.5	68.5	96.3	85.8	62.4	69.8	56.4	96.8	88.3		
	OE(%)	0.0	6.3	5.5	31.5	3.7	15.2	37.6	30.2	43.6	3.2	11.7		

Table 5. Comparison of clustering algorithms

K-means	Cluster membership is influenced by computing the centroid for every group and conveying every object to the group with the neighbouring centroid.	Iteration of reallocation of cluster members is reduced by the total with-in cluster scattering.
Hierarchical clustering	It divides or combines previous groups, a hierarchical structure is created which reflects the arrangement in which groups are separated or mingled.	It is more adaptable and eases to handle.
Self-Organization map algorithm	This algorithm found a good mapping from 2-D representation to high dimensional input space. An objects in the same space constituted by the similar node as sorted into a cluster.	It is used to shape the big clusters and also used for speech recognition and vector quantization.
SVD trace algorithm	It converts the connected variables into a group of uncorrelated ones that well again rendering the different relationships between the original data items. At the same time, SVD is a method for ordering and identifying the dimensions beside which data points reveal a large amount of variation.	It gives more accuracy than other methods.

Table 6. Comparison of unsupervised classification algorithm

MLC	They create relative high accuracies using a smaller sized training set and accomplish stable results when there are 60 or more samples/ class.	It improves accuracy and performance level is high.
ANN Classification	It is based on the presentation pattern of the input vector for little amount of training data therefore, the training patterns are accessible in sequence to the Neural Networks	It improves the performance by training and proper attention.
Proposed EML algorithm	The single decisions of the clusters were not considered, while group decisions of all the samples are taken into account. The weighted averaging and classification for regression is improved by MPF technique.	It minimizes error when compared to previous techniques.

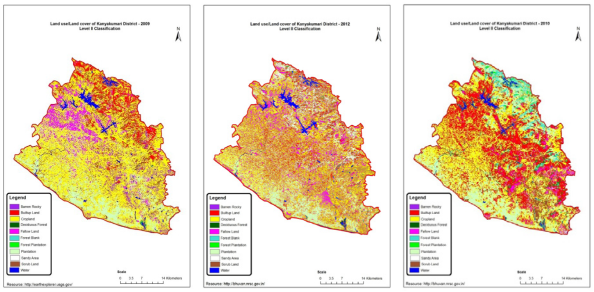

Figure 4. Land use/land cover classification of Landsat-8. Liss 3, AWiFS.

6. Conclusion

These results are enormously important for agricultural department services. The above results are based on the incorporation of LANDSAT-8, Liss-3 and AWFIS images. This study is mainly concentrated on the district of Kanyakumari, Tamil Nadu, India. The land use/land cover patterns is taken into account in this study. The topographical images were taken and the features can be extracted by using LSBFE algorithm which gives 89% accuracy and the extracted image is clustered into a group to avoid imbalance clusters by using SVD trace algorithm and the accuracy is improved to 90.5%. Then, the image is classified to achieve better minimization of error by using EML classification algorithm and improves 91% accuracy. By the various proposed algorithm, we get better and clear images of land use/land cover patterns and higher accuracy when compared to previous methods. The overall accuracy of Landsat-8 shows 92.5% accuracy, for Liss-3 shows 89.6% accuracy and AWFIS shows 89.5% accuracy. In future, we can apply the above mentioned novel feature extraction and clustering algorithm for change detection analysis, forest degradation analysis etc.

7. References

1. Chellasamy M, Ferre TPA, Greve MH. An ensemble-based training data refinement for automatic crop discrimination using worldview-2 imagery. IEEE Journal of Selected Topics in Applied Earth Observations and Remote Sensing. 2015; 8(10):4882–94.
2. Skakun S, Kussul N, Shelestov AY, Lavreniuk M, Kussul O. Efficiency assessment of multitemporal C-band Radarsat-2 intensity and Landsat-8 surface reflectance satellite imagery for crop classification in Ukraine. IEEE Journal of Selected Topics in Applied Earth Observations and Remote Sensing. 2015; 9(8):3712–9.
3. Ozdemir D, Akarun L. Fuzzy algorithms for combined quantization and dithering. IEEE Transactions on Image Processing. 2001; 10(6):923–31.
4. Zhang X, Liao C, Li J. Sun fractional vegetation cover estimation in arid and semi-arid environments using HJ-1 satellite hyperspectral data. International Journal of Applied Earth Observation and Geoinformation. 2013; 21:506–12.
5. Hao M, Shi W, Zhang H, Li C. Unsupervised change detection with expectation-maximization-based level set. IEEE Geoscience and Remote Sensing Letters. 2014; 11(1):210–4.
6. Jia K, Wu B, Tian Y, Zeng Y, Li Q. Vegetation classification method with biochemical composition estimated from remote sensing data. International Journal of Remote Sensing. 2011; 32(24):9307–25.
7. Jia K, Liang S, Wei, Zhang X, Yao L, Gao YS. Automatic land-cover update approach integrating iterative training sample selection and a Markov Random Field model. Remote Sensing Letters. 2014; 5(2):148–56.
8. Xiao Z, Liang S, Wang J, Chen P, Yin X, Zhang L, Song J. Use of general regression neural networks for generating the GLASS leaf area index product from time-series MODIS surface reflectance. IEEE Transactions on Geoscience and Remote Sensing. 2014; 52(1):209–23.
9. Jiapaer G, Chen X, Bao A. A comparison of methods for estimating fractional vegetation cover in arid regions. Agricultural and Forest Meteorology. 2011; 151(12):1698–710.
10. Miao Q, Xu P, Liu T, Song J, Chen X. A novel fast image segmentation algorithm for large topographic maps. Neurocomputing. 168; 808–22.
11. Huang G, Song S, Gupta JN, Wu C. Semi-supervised and unsupervised extreme learning machines. IEEE Transactions on Cybernetics. 2012; 44(12):2405–17.
12. Qin C, Song S, Huang G, Zhu L. Unsupervised neighbourhood component analysis for clustering. Neurocomputing. 2015; 168:609–17.
13. Klaric MN, Claywell BC, Scott GJ, Hudson NJ, Sjahputera O, Li Y, Davis CH. GeoCDX: An automated change detection and exploitation system for high-resolution satellite imagery. IEEE Transactions on Geoscience and Remote Sensing. 2013; 51(4):2067–86.
14. Sun W, Heidt V, Gong P, Xu G. Information fusion for rural land-use classification with high-resolution satellite imagery. IEEE Transactions on Geoscience and Remote Sensing. 2003; 41(4):883–90.
15. Saitwal K, Azimi-Sadjadi MR, Reinke D. A multichannel temporally adaptive system for continuous cloud classification from satellite imagery. IEEE Transactions on Geoscience and Remote Sensing. 2003; 41(5):1098–104.
16. Zhang Y, Guindon B. Quantitative assessment of a haze suppression methodology for satellite imagery: Classification

performance. IEEE Transactions on Geoscience and Remote Sensing. 2003; 41(5):1082–9.

17. Pacifici F, Frate D, Solimini F, Emery CWJ. An innovative neural-net method to detect temporal changes in high-resolution optical satellite imagery. IEEE Transactions on Geoscience and Remote Sensing. 2007; 45(9):2940–52.
18. Mukhopadhyay A, Maulik U. Unsupervised pixel classification in satellite imagery using multiobjective fuzzy clustering combined with SVM classifier. IEEE Transactions on Geoscience and Remote Sensing. 2009; 47(4):1132–8.
19. Salmon BP, Kleynhans W, Den Bergh V, Olivier FJC, Grobler TL, Wessels KJ. Land cover change detection using the internal covariance matrix of the extended Kalman filter over multiple spectral bands. IEEE Journal of Selected Topics in Applied Earth Observations and Remote Sensing. 2013; 6(3):1079–85.
20. Cheriyadat AM. Unsupervised feature learning for aerial scene classification. IEEE Transactions on Geoscience and Remote Sensing. 2014; 52(1):439–51.
21. Yousif O, Ban Y. Improving urban change detection from multitemporal SAR images using PCA-NLM. IEEE Transactions on, Geoscience and Remote Sensing. 2013; 51(4):2032–41.
22. Ghosh A, Subudhi BN, Bruzzone L. Integration of Gibbs Markov random field and Hopfield-type neural networks for unsupervised change detection in remotely sensed multitemporal images. IEEE Transactions on Image Processing. 2013; 22(8):3087–96.
23. Menaka E, Kumar SS, Bharathi BM. Change detection in deforestation using high resolution satellite image with Haar wavelet transforms. IEEE International Conference on Green High Performance Computing (ICGHPC); India. 2013. p. 1–7.
24. Hendrickx M, Laet D, Stal VC, Wulf D, Goossens AR. The use of high resolution digital surface models for change detection and viewshed analysis in the urban area around the pyramids of Giza, Egypt. IEEE proceedings on Urban Remote Sensing Event (JURSE); Belgium. 2013. p. 021–4.
25. Netzband M, Kirschberg C. Urban change detection by means of multitemporal satellite imagery- The case of the Indian mega-city Hyderabad. IEEE on Urban Remote Sensing Event (JURSE); Germany. 2013. p. 182–5.
26. Brett PT, Guida R. Earthquake damage detection in urban areas using curvilinear features. IEEE Transactions on Geoscience and Remote Sensing. 2013; 51(9):4877–84.
27. Sahbi H. Relevance feedback for satellite image change detection. IEEE International Conference on Acoustics, Speech and Signal Processing (ICASSP); India. 2013. p.1503–7.
28. Sulaiman NA, Ruslan FA, Tarmizi MDN, Hashim KA, Samad AM. Mangrove forest changes analysis along Klang coastal using remote sensing technique. IEEE 3rd International Conference on System Engineering and Technology (ICSET); Delhi. 2013. p. 307–12.
29. Leigh S, Wang Z, Clausi DA. Automated ice–water classification using dual polarization SAR satellite imagery. IEEE Transactions on Geoscience and Remote Sensing. 2014; 52(9):5529–39.
30. Hoberg T, Rottensteiner F, Feitosa QR, Heipke C. Conditional random fields for multitemporal and multiscale classification of optical satellite imagery. IEEE Transactions on Geoscience and Remote Sensing. 2015; 53(2):659–73.
31. Fernandez I, Aguilar FJ, Aguilar MA, Alvarez FM. Influence of data source and training size on impervious surface areas classification using VHR satellite and aerial imagery through an object-based approach. IEEE Journal of Selected Topics in Applied Earth Observations and Remote Sensing. 2014; 7(12):4681–91.
32. Yuan Y, Hu X. Bag-of-words and object-based classification for cloud extraction from satellite imagery. IEEE Journal of Selected Topics in Applied Earth Observations and Remote Sensing. 2015; 8(8):4197–205.
33. Wu KL, Yang MS. Alternative c-means clustering algorithms. Pattern Recognition. 2002; 35(10):2267–78.
34. Ozdemir D, Akarun L. A fuzzy algorithm for color quantization of images. Pattern Recognition. 2002; 35(8):1785–91.
35. Pippuri I, Suvanto A, MaltamoM, Korhonen KT, Pitkanen J, Packalen P. Classification of forest land attributes using multi-source remotely sensed data. International Journal of Applied Earth Observation and Geoinformation. 2016; 44:11–22.
36. Vignesh T, Thyagharajan KK. Local binary pattern texture feature for satellite imagery classification. International Conference on Science, Engineering and Management Research; India. 2014. p.1–6.
37. Vignesh T, Thyagharajan KK. Efficient classification methodology for change detection using satellite imagery. Australian Journal of Basic and Applied Sciences. 2015; 9(20):580–90.
38. Banu JS, Babu R, Pandey R. Parallel implementation of Singular Value Decomposition (SVD) in image compression using open mp and sparse matrix representation. Indian Journal of Science and Technology. 2015 Jul; 8(13):1–10.
39. Prasad KL, Rao TM, Kannan V. A novel and hybrid secure digital image watermarking framework through sc-LWT-SVD. Indian Journal of Science and Technology. 2016 Jun; 9(23):1–10.
40. Van-Tu N, Cuong L. Improving question classification by feature extraction and selection. Indian Journal of Science and Technology. 2016 May; 9(17):1–8.
41. Jayasri T, Hemalatha M. Categorization of respiratory signal using ANN and SVM based on feature extraction algorithm. Indian Journal of Science and Technology. 2013 Sep; 6(9):1–6.